J Mater Sci (2010) 45:2967–2973
DOI 10.1007/s10853-010-4294-x

Fabrication and growth mechanism of hexagonal zinc oxide nanorods via solution process

Rizwan Wahab · Young-Soon Kim · Kyeongseop Lee · Hyung-Shik Shin

Received: 14 December 2009 / Accepted: 2 February 2010 / Published online: 17 February 2010

Abstract This article presents, the fabrication of perfectly hexagonal zinc oxide nanorods performed via solution process using zinc nitrate hexahydrate ($Zn(NO_3)_2{\cdot}6H_2O$) and hexamethylenetetramine (HMT) at various concentrations of i.e. 1×10^{-3} to 10×10^{-2} M in 50 mL distilled water and refluxed at 100 °C for 1 h. We used HMT because it acts as a template for the nucleation and growth of zinc oxide nanorods, and it also works as a surfactant for the zinc oxide structures. The X-ray diffraction patterns clearly reveal that the grown product is pure zinc oxide. The diameters and lengths of the synthesized nanorods lie in the range of 200–800 nm and 2–4 μm, respectively as observed from the field emission scanning electron microscopy (FESEM). The morphological observation was also confirmed by the transmission electron microscopy (TEM) and clearly consistent with the FESEM observations. The chemical composition was analyzed by the FTIR spectroscopy, and it shows the ZnO band at 405 cm^{-1}. On the basis of these observations, the growth mechanism of ZnO nanostructures was also proposed.

Introduction

It is difficult to fabricate and control the nanostructures to their own size and shape in the material science. Lot of efforts have been made toward this direction to tune the shape and size of nanocrystals because nano-crystalline materials are technologically important because of their optical, electrical, and other properties [1–3]. Till date, a variety of semiconductor nanostructures have been synthesized and reported in the literature with their practical applications dependent on their structural properties [4]. Among the various semiconductor nanostructures, zinc oxide exhibits a variety of nanostructures, and, hence, it is believed that it is the richest group of nanostructures [5]. It has a wide band gap (3.37 eV) and large exciton-binding energy of about 60 meV at room temperature and has many applications in the field of optoelectronic devices, such as for light emitting diodes, field-effect transistors, ultra violet nanolasers, solar cells, and acoustic electrical devices gas sensors [6–8]. Wang and co-workers have reported many types of nanostructures of zinc oxide such as nanowires, nanobelts, nanobridges, nanonails, nanoribbons, nanorods, nanotubes, and whiskers by the thermal evaporation of zinc powder and hydrothermal synthesis [9–11]. Metal organic chemical vapour deposition (MOCVD), spray pyrolysis, ion beam-assisted deposition, laser-ablation, sputter deposition, template-assisted growth, and chemical vapour deposition are usually employed for the synthesis of zinc oxide nanostructures [12–15]. Among these techniques, preparation of zinc oxide via a solution chemical route provides an easy and convenient method and is very effective for the large-scale production of nanocrystals. It is known that zinc oxide is a polar crystal, where the zinc and oxygen ions are arranged alternatively along the *c*-axis direction in a hexagonal structure. The growth habit of zinc oxide is mainly dependent on the internal structure, but it is also affected by the external conditions such as reaction temperature, reaction concentration, and the pH of the solution [16]. Previously, Gao et al. reported the formation of flower-like ZnO nanostructures on a silicon substrate at 95 °C in 12 h by the decomposition of an ehthylenediamine–zinc complex with the assistance of hexamethylenetetramine (HMT) in a

R. Wahab · Y.-S. Kim · K. Lee · H.-S. Shin (✉)
Energy Materials & Surface Science Laboratory, Solar Research Center, School of Chemical Engineering, Chonbuk National University, Jeonju 561-756, Republic of Korea
e-mail: hsshin@chonbuk.ac.kr

laboratory Pyrex glass bottle with polypropylene autoclavable screw caps and with a filling ratio of 80% [17]. Ahsanulhaq et al. reported the synthesis of ZnO nanowires using water soluble HMT and zinc nitrate hexa-hydrate via solution method at 95 °C in 16 h refluxing. [18]. In another article, Kar et al. presented the synthesis of zinc oxide nanostructures at various dimensions using pattern substrates by HMT and Zinc nitrate hexa-hydrate via solution method at 75 °C in 8 h via hydrothermal method [19]. The assembly of ZnO nanorods was synthesized by HMT and zinc nitrate hexa-hydrate via hydrothermal method at 95 °C in different time (10–50 h) intervals [20].

In all the results reported above, the nanostructures were grown either in long refluxing time, or they needed sophisticated instruments and complex reaction procedures for the growth of nanostructure of zinc oxide. In this article, we report an easy and low cost approach for the synthesis of hexagonal zinc oxide nanorods at ~100 °C via solution method using zinc nitrate hexa-hydrate and HMT in a short refluxing time. Here, we observed that the morphology of zinc oxide nanorods changes by only varying the concentration of HMT. The synthesized products are highly crystalline and exhibit good optical and chemical properties. Therefore, our synthetic approaches provide a simple, cost-effective, easy, and convenient route to obtain large quantities of hexagonal zinc oxide nanorods. The mechanism of formation of zinc oxide nanorods is also discussed.

Experimental

Material synthesis

Zinc oxide hexagonal nanorods were successfully synthesized using zinc nitrate hexahydrate ($Zn(NO_3)_2{\cdot}6H_2O$) and HMT ($(CH_2)_6N_4$). In a typical experiment, 0.3 M zinc nitrate hexahydrate ($Zn(NO_3)_2{\cdot}6H_2O$) was dissolved in 50 mL of distilled water at various concentrations of i.e. 1×10^{-3} to 10×10^{-2} M in 50 mL distilled water and refluxed at 100 °C for 1 h. The obtained solution was stirred for 30 min for the complete dissolution. Zinc nitrate hexahydrate ($Zn(NO_3)_2{\cdot}6H_2O$) and HMT were purchased for this experiment from Aldrich chemical corporation and used without further purification. Solution pH was measured by the expandable ion analyzer (EA 940, Orian made from UK), and it was found that the pH of the solution was reached at ~6.7. After the complete dissolution, the mixture was transferred to the three-necked refluxing pot and refluxed at 100 °C for 1 h. The precipitate was observed when the temperature raises at 100 °C but for the complete precipitation, the solution was refluxed for 1 h. The refluxing temperature was measured and controlled by k-type thermocouple and a PID temperature controller. While refluxing, the pH of the solution was neither measured nor controlled. After refluxing, the white powder was washed with methanol several times and dried at room temperature. The obtained as grown powder was examined in terms of their structural and chemical properties.

Characterizations

The morphological characterizations were obtained by using field emission scanning electron microscopy (FESEM) and transmission electron microscopy (TEM). For SEM observation, the powder was uniformly sprayed on carbon tape. In order to avoid charging while observation, the powder was coated by the thin osmium oxide (OsO_4) for 5 s. For the transmission electron microscopic measurement, powder was sonicated in ethanol for 10 min by dipping copper grid in the solution and drying at room temperature. The crystallinity and crystal phases of as-grown powder so obtained was determined using X-ray powder diffractometer (XRD) $Cu_{K\alpha}$ radiation ($\lambda = 1.54178$ Å), Bragg angle ranging from 20° to 65° with 8°/min scanning speed. The composition of the synthesized ZnO nanostructures were characterized by the Fourier transform infrared (FTIR) spectroscopy in the range of 400–4000 cm^{-1}. In addition to this, the optical property of synthesized material was also studied by the UV–visible (UV–vis) absorption double beam spectrophotometer with a deuterium and tungsten iodine lamp in the range from 200 to 800 nm at room temperature. The powder sample was dispersed in the de-ionized water and sonicated for 10 min for the complete dispersion of the sample.

Results and discussion

X-ray diffraction analysis

Figure 1 shows the X-ray diffraction spectrum of microflowers composed with hexagonal zinc oxide nanorods synthesized at ~100 °C in 1 h refluxing, which shows a typical spectrum of synthesized ZnO. The observed diffraction peaks are well-matched with the typical single crystalline wurtzite hexagonal phase bulk ZnO (JCPDS, Card No. 36-1451). No other peaks were detected within the detection limit of the X-ray diffraction instrument. The intense and sharp peaks in the diffraction spectrum show the high-crystallinity of the as-synthesized products.

Morphological observations (FESEM result)

Figure 2 shows the general morphology and bar graph of diameter and length with respect to increasing concentration of HMT (1×10^{-3} to 10×10^{-2} M) using solution of

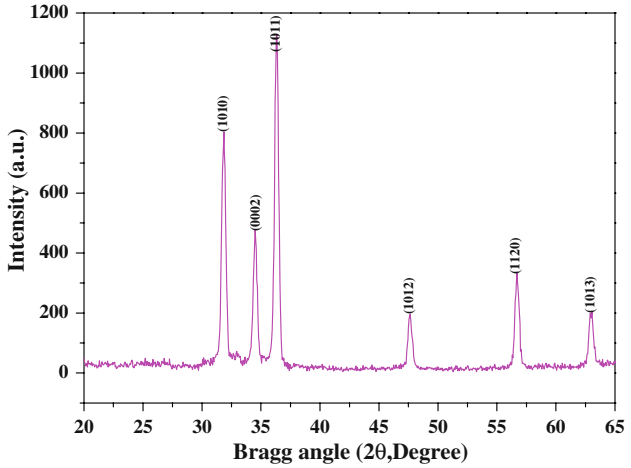

Fig. 1 Typical X-ray diffraction pattern of as synthesized hexagonal ZnO nanorods

Zinc nitrate hexahydrate ($Zn(NO_3)_2{\cdot}6H_2O$) in double deionized distilled water at 100 °C refluxing for 1 h. Figure 2a–l shows the FESEM images of synthesized powder at $Zn(NO_3)_2{\cdot}6H_2O$ (0.3 M): HMT (1×10^{-3} to 10×10^{-2} M) concentration, where the full micro-flower types zinc oxide nanorods can be seen. The typical lengths of the grown nanorods are in the range of 2–4 μm, where as the diameter of each nanorods varies form 200–800 nm with increasing concentration of HMT (Fig. 2m–n). The nanorods are joined together to form a micro-flower type structure of zinc oxide. The surface of each nanorod is smooth, clean, and of hexagonal structure. When the synthesis process was carried out at higher concentration of HMT-$Zn(NO_3)_2{\cdot}6H_2O$ (0.3 M): HMT (5×10^{-3} to 6×10^{-3} M) at 100 °C refluxing temperature in 60 min., the surface of nanorods changes hexagonal to circular in shape as well as the length and diameter of nanorods decreases. In addition, the micro-flower-shaped structures are formed by the accumulation of several hundreds of hexagonal ZnO-nanorods. It is clearly seen from the images that all the nanorods originated from a single center and are arranged in such a manner that they are exhibiting a spherical flower-like morphologies. All the ZnO nanorods are joined together through their wider bases in a spherical shape for forming the flower-shaped structures. The full array of one flower-shaped structure is in the range of 2–3 μm. We found in our experiment that for the concentrations HMT at 1×10^{-2}, 2×10^{-2}, 6×10^{-2}, 7×10^{-2}, and 8×10^{-2} M, the surface of nanorods becomes rough and thick in nature, whereas for concentrations at 3×10^{-2}, 4×10^{-2}, 5×10^{-2}, and 10×10^{-2} M of HMT, the surface of nanorods are smooth and clean with hexagonal shape. Here, the growth of each nanorod increases in vertical direction [2110] rather in longitudinal or *c*-axis direction [0001] [21]. From FESEM images, we can easily see that the shapes of hexagonal ZnO-nanorods are dependent on the concentration of HMT, and we can modify and control the shape and size of ZnO-nanorods by suitable choice of HMT concentration.

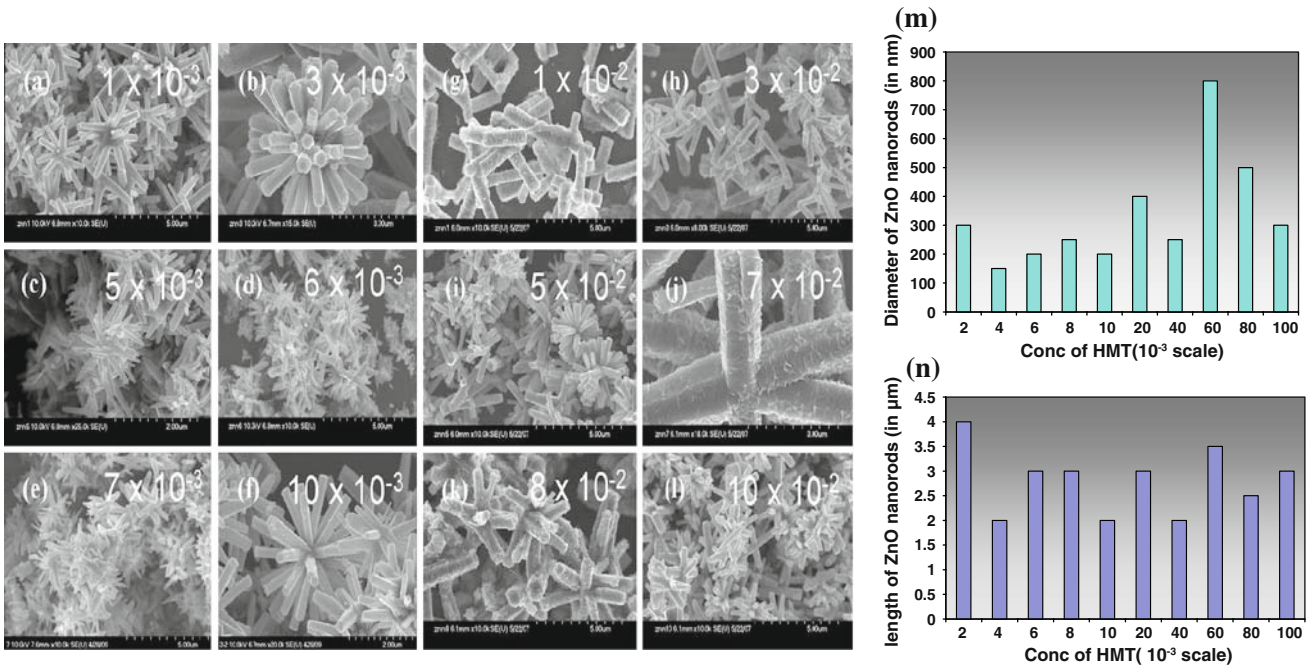

Fig. 2 FESEM images of zinc oxide nanorods at different (low and high) concentrations of HMT (**a**–**l**) and their bar graph showing the (**m**) diameter and (**n**) length respectively

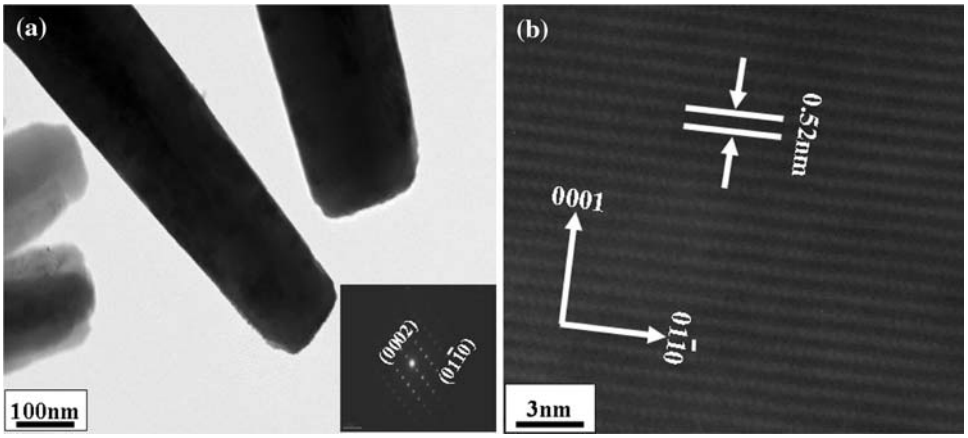

Fig. 3 **a** Low magnification TEM image of the hexagonal ZnO-nanorods at 0.3 M concentration of zinc nitrate hexa-hydrate and hexamethylenetertamine (HMT). **b** HR-TEM image shows the difference between two lattice fringes, which is about 0.52 nm. The corresponding SAED pattern ((**a**) *inset lower side*) is clearly consistent with the HR-TEM observations and indicates the synthesized product is wurtzite hexagonal zinc oxide

TEM results

The structural morphology of the synthesized hexagonal zinc oxide nanorods was further characterized via TEM equipped with the selected area electron diffraction (SAED) patterns. Figure 3a shows the low magnification TEM image of the ZnO nanorods grown via solution process in refluxing pot at 100 °C for 1 h. The TEM image is clearly consistent with the FESEM observations and reveals that the formed nanorods have sharpened hexagonal morphology with the wider bases. The base diameters of the obtained nanorods are in the range of 150–200 nm. Moreover, the nanorods are exhibiting smooth and clean surfaces throughout their length. The corresponding SAED pattern obtained from the shown nanorods confirmed that the synthesized products are single crystalline and grow along the [0001] direction (inset lower side (a)). Figure 3b shows the high resolution TEM (HR-TEM) image of the corresponding nanorods. The lattice fringes between two adjacent plane was about 0.52 nm which is equal to the lattice constant of the ZnO and indicates that the obtained structure has a wurtzite hexagonal phase, and are preferentially grown along the *c*-axis [0001] direction. The corresponding SAED pattern is consistent with the HR-TEM observations and further confirms that the obtained nanostructures are single crystalline with the wurtzite hexagonal phase and grown along the [0001].

Compositional and optical analysis (FTIR spectroscopy results)

The functional or composition quality of the synthesized product was analyzed by the FTIR spectroscopy. Figure 4 shows the FTIR spectrum which was acquired in the range

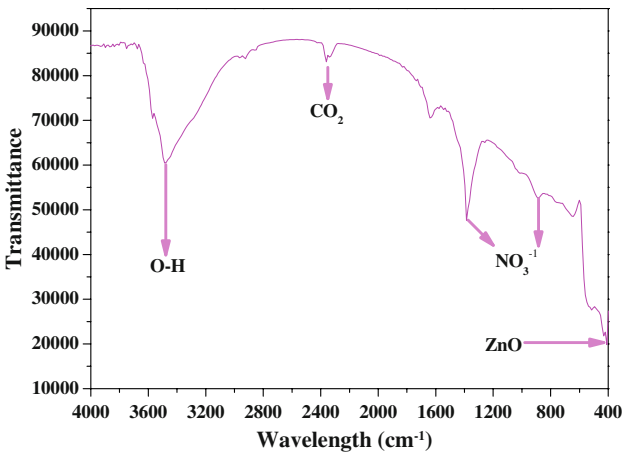

Fig. 4 Typical FTIR spectrum of as grown hexagonal ZnO-nanorods

of 400–4000 cm^{-1}. The band at 405 cm^{-1} is correlated to zinc oxide [22] where as the bands at 3200–3600 cm^{-1} correspond to O–H mode of vibration. The small asymmetric stretching mode of vibration of O–H was observed at 1629 cm^{-1}. The symmetric stretching occurring between 1385 and 887 cm^{-1} indicates the vibration of NO_3^{-1} ions [23–26].

The optical property of as-synthesized zinc oxide nanorods was examined by UV–vis spectroscopy at room temperature as demonstrated in Fig. 5. UV–vis spectroscopy is the measurement of the absorption of near and visible ultraviolet light using semiconductor zinc oxide nanostructures. In our zinc oxide nanostructures, sample gives an electronic transition at specific wavelengths that are absorbed and intensity of the absorption gives us information about the electronic spectra of the sample. The nanostructures wave length was found to be ~360 nm,

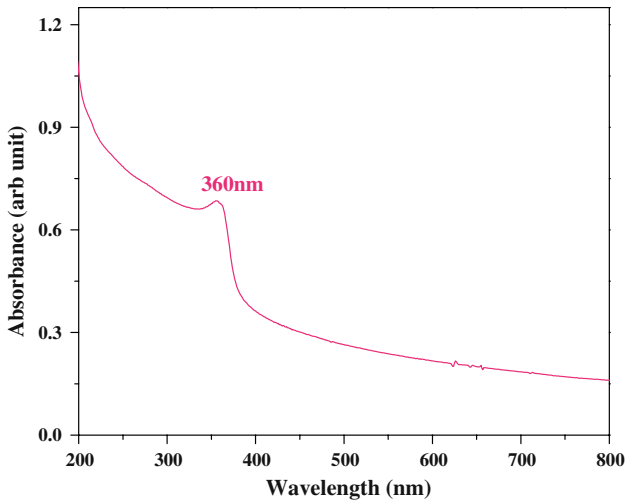

Fig. 5 Typical UV–vis spectra of synthesized ZnO nanorods

which is a characteristic peak of wurtzite hexagonal phase of ZnO, demonstrating that the synthesized products are pure ZnO [21, 24]. We found that the band gaps (~3.44 eV) of our synthesized nanostructures are very near to the available band gap of bulk ZnO (~3.37 eV) [21, 24]. Owing to the presence of a broad peak in the obtained UV–vis spectra, one can easily conclude that the grown ZnO nanostructures exhibit good optical property containing wurtzite hexagonal phase.

Possible growth mechanism for hexagonal zinc oxide nanorods

On the basis of microscopic results, we can easily predict the possible growth mechanism for the formation of hexagonally shaped zinc oxide nanorods by the variation of HMT solution concentration. The growth of zinc oxide nanorods comprises two steps: nucleation of small molecules, and its growth/fabrication of matured hexagonally shaped nanorods. When an aqueous solution of zinc salt ($Zn(NO_3)_2{\cdot}6H_2O$) reacts, compounds with low solubility are precipitated out of the solutions. This study demonstrates the formation of hexagonally shaped ZnO nanorods formed using zinc nitrate hexa-hydrate ($Zn(NO_3)_2{\cdot}6H_2O$) and HMT ($C_6H_{12}N_4$). The generation of OH^- (hydroxyl ions) was produced from HMT, and it is extensively used in the fabrication of ZnO nanostructures. When the HMT reacts with water, it produces ammonia. The ammonia further reacts with water molecule and forms ammonium (NH_4^+) ions in the solution. As we know that in solution, Zn^{2+} ions can largely react with the four molecules of ammonia (NH_3) and forms tetrahedral complexes of zinc ($(Zn(NH_3)_4^{2+}$). In our case, four hydroxyl ions of ammonia react with the Zn^{2+} and form building blocks of zinc ammonium complex $Zn(NH_3)_4^{2+}$, and when the refluxing temperature increases, the four coordinated complex ions changes to ZnO, ammonia, and water molecule. The formation of ZnO can be represented as the following reactions.

$$(CH_2)_6N_4 + 6H_2O \rightarrow 6HCHO + 4NH_3 \quad (1)$$

$$NH_3 + H_2O \rightarrow NH_4^+ + OH^- \quad (2)$$

$$Zn^{2+} + 4NH_3 \rightarrow Zn(NH_3)_4^{2+} \quad (3)$$

$$H_2O \rightarrow H^+ + OH^- \quad (4)$$

$$2OH^- + Zn(NH_3)_4^{2+} \rightarrow ZnO + 4NH_3 + H_2O \quad (5)$$

In solution, the colloidal precipitates of $Zn(OH)_2$ were further dissociated into Zn^{2+} and OH^- ions in the presence of water and thermal energy (i.e., while refluxing). It is expected that when the concentrations of these Zn^{2+} and OH^- ions exceed the critical value, the precipitation of ZnO nuclei starts. One can call this process as the initial nucleation process for the formation of ZnO. Solution technique is a pH-sensitive technique where material properties can be tailored e.g., by changing the concentration of OH^- ions refluxing temperature. A detailed experiment is needed to understand the influence of these parameters. In this study, only the variation of concentration of HMT was used as a control parameter to change the structure/morphology of ZnO, and hence the changes in Zn^{2+} and OH^- ions can be correlated to the increase in thermal energy of the system. Raising the refluxing bath temperature promotes the dissociation of the zinc complex ($Zn(OH)_2$) and leads to the controlled release of free zinc ions (Zn^{2+}) and hydroxide ions (OH^-). The following reaction occurs immediately:

$$Zn(OH)_2 \rightarrow Zn^{2+} + 2OH^-. \quad (I)$$

$$Zn^{2+} + 2OH^- \rightarrow ZnO + H_2O. \quad (II)$$

The transformation from zinc complex ($Zn(NH_3)_4^{2+}$) to ZnO is a kinetic-controlled growth process. The aggregation of ZnO competes with the nucleation to modify the final particle size or shape. In this experimental case, HMT behaves as a template/capping molecule for the growth of hexagonal zinc oxide nanorods. It is assumed that the initially formed $Zn(OH)_2$ and $Zn(NH_3)_4^{2+}$ nuclei get aggregated (Fig. 6a, b) and after acquiring sufficient thermal energy from the refluxing pot, they form a core sphere and provide a suitable energy for the attachment of active molecules of ZnO. The active ZnO nuclei thus formed are expected to be the building blocks for the formation of the final product. These active molecules are generally referred to as primary stems and form in hexagonal shapes which are attached on the core cells of the zinc oxide (Fig. 6c–g). Once the flower stems

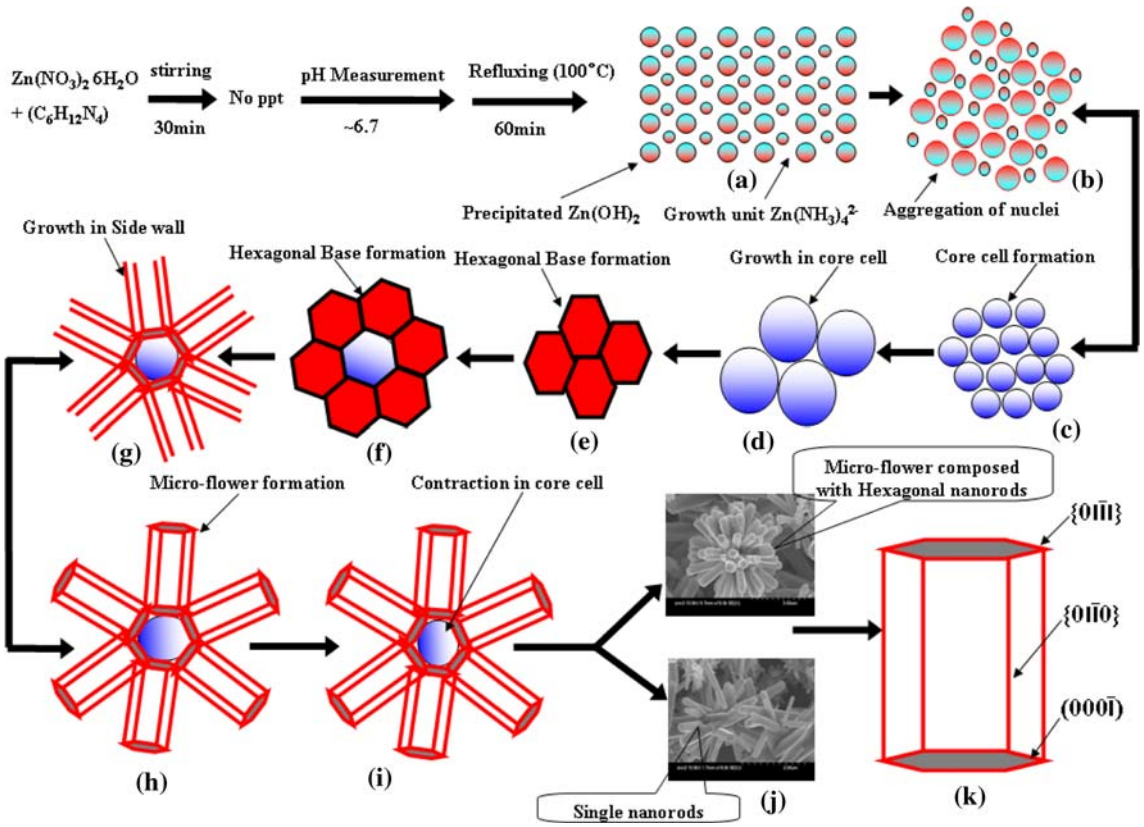

Fig. 6 Typical growth mechanism for the fabrication of micro-flower composed with hexagonal nanorods: nuclei (**a**, **b**), core cell (**c**, **d**), hexagonal base (**e**, **f**), micro-flower (**g**–**i**), images of single and micro-flower composed with hexagonal nanorods formation steps

are formed on the surface of the core cells, they grow in a linear direction and, based on surface energy considerations, rearrange themselves into a complete micro-flower structure (Fig. 6h). After forming the micro-flower structure, the core shells undergoes contraction with energy, and the matured micro-flower composed with hexagonal zinc oxide nanorods can be seen (Fig. 6i–k). The small petals with six defined facets arise to maintain a minimum in the surface energy so as to retain the symmetry of the crystal structure (wurtzite ZnO). It is well known that the radii of a newly formed crystal increases linearly with time after the formation of a nucleus. As new crystals grow, their boundaries also move at a given speed and eventually touch each other, forming the base of the structure. Once the base is formed, the growth rate starts to decrease along the transverse direction and growth in the radial direction continues with the top surface, an energetically favored surface [23–26].

Conclusions

We presented here a systematic study of concentration variation using zinc nitrate hexahydrate ($Zn(NO_3)_2 \cdot 6H_2O$) and HMT ($C_6H_{12}N_4$) and found that the morphology of ZnO nanostructures depends on the concentration HMT ($C_6H_{12}N_4$) of the precursor solution. On the basis of microscopic (FESEM and TEM) studies, we can easily conclude that the size/morphology of the structure depends on the variation of concentration. On the other hand, the crystallinity and compositional analysis indicated that the solution concentration does not impact much on the quality of the material as observed from X-ray diffraction pattern and FTIR spectroscopy. In addition, the optical property (UV–vis spectroscopy) of grown sample shows good optical property as compared to bulk ZnO.

Acknowledgements We acknowledge the support received from the Korean Federation of Science and Technology (KOFST) and KRF fellowship in the form of KOSEF research grant no. R01-2007-000-20810-0 and KMOST research grant no. 2004-01352. We would also like to thank Mr. Kang Jong-Gyun, Center for University-wide Research Facilities, Chonbuk National University for his cooperation in TEM observations, and the Korea Basic Science Institute, Jeonju branch, for letting us use their FESEM facility.

References

1. Duan X, Huang Y, Agarwal R, Lieber CM (2003) Nature 421:241
2. Hung MH, Mao S, Feick H, Yan H, Wu Y, Kind WE, Russo R, Yang P (2001) Science 292:1897
3. Michal DW (2000) Nature 405:293

4. Beek WJE, Wienk MM, Emerink MK, Yang X, Janssen RAJ (2005) J Phys Chem B 109:9505
5. Wang ZL (2004) Mater Today 7:26
6. Chen Y, Bangall DM, Koh H, Park K, Hiraga K, Zhu Z, Yao T (1998) J Appl Phys 84:3912
7. Wu Y, Yan H, Huang M, Messer B, Song JH, Yang P (2002) Chem Eur J 8:1260
8. Sberveglieri G, Groppelli S, Nelli P, Tintinelli A, Giunta G (1995) Sens Actuators B 24–25:588
9. Pan WZ, Dai RZ, Wang ZL (2001) Science 291:1947
10. Lao JY, Huang JY, Wang DZ, Ren ZF (2003) Nano Lett 3(2):235
11. Zahang H, Deren Y, Li D, Ma X, Li S, Que D (2005) Cryst Growth Des 5:547
12. Haga K, Katahira F, Watanabe H (1999) Thin Solid Films 343:145
13. Studenikin SA, Golego N, Cocivera M (1998) J Appl Phys 84:2287
14. Sun Y, Fuge GM, Ashfold MNR (2004) Chem Phys Lett 396:21
15. Li Y, Meng GW, Zhang LD (2000) Appl Phys Lett 76:2011
16. Sekiguchi T, Haga K, Inaba K (2000) J Cryst Growth 214/215:68
17. Gao X, Li X, Yu W (2005) J Solid State Chem 178:1139
18. Ahsanulhaq Q, Kim SH, Hahn YB (2009) J Phys Chem Solids 70:627
19. Kar JP, Ham MH, Lee SW, Myoung JM (2009) Appl Surf Sci 255:4087
20. Gao YJ, Zhang WC, Wua XL, Xia Y, Huang GS, Xu LL, Shen JC, Siu GG, Paul KC (2008) Appl Surf Sci 255:1982
21. Polsongkram D, Chamninok P, Pukird S, Chow L, Lupan O, Chai G, Khallaf H, Park S, Schulte A (2008) Physica B 403:3713
22. Wahab R, Ansari SG, Kim YS, Seo HK, Kim GS, Khang G, Shin HS (2007) Mater Res Bull 42:1640
23. Wahab R, Ansari SG, Kim YS, Seo HK, Shin HS (2007) Appl Surf Sci 253:7622
24. Wahab R, Ansari SG, Kim YS, Khang G, Shin HS (2008) Appl Surf Sci 254:2037
25. Wahab R, Ansari SG, Seo HK, Kim YS, Suh EK, Shin HS (2009) Solid State Sci 11:439
26. Wahab R, Kim YS, Shin HS (2009) Mater Trans 8:2092